

Numerical study of the spin-3/2 Ashkin-Teller model

R. Boudefla^{1*}, S. Bekhechi¹, F. Hontinfinde²

¹ Laboratoire de Physique Théorique (LPT), B.P. 230, Université Abou Bekr Belkaïd, Tlemcen 13000, Algeria

² Département de Physique (FAST) et Institut des Mathématiques et de Sciences Physiques (IMSP), Université d'Abomey-Calavy, 01 B.P. 613, Porto-Novo, Benin

Received November 8, 2014, in final form May 10, 2015

The study of the Ashkin-Teller model (ATM) of spin-3/2 on a hypercubic lattice is undertaken via Monte Carlo simulation. The phase diagrams are displayed and discussed in the physical parameter space. Rich physical properties are recovered, namely the second order transition and multicritical points. The phase diagrams have been obtained by varying the strength describing the four spin interaction and the single ion potential. This model shows a new high temperature partially ordered phase, called $\langle S \rangle$ and a new Baxter 3/2 ground state which do not exist either in the spin-1/2 ATM or in the spin-1 ATM.

Key words: modelization, Ashkin-Teller, spin-3/2, Monte-Carlo, phase diagram, Baxter

PACS: 75.10.Hk

1. Introduction

In this work, we will analyze a magnetic model with three spin states known as Ashkin-Teller model [1] which is a superposition of two Ising models with spin variables σ and S . In every site i of the cubic lattice, two spin variables σ_i and S_i are associated. In each Ising model, there are two spin nearest-neighbors interaction with a strength K_2 [2]. In addition, different Ising models are coupled by a four-spin interaction with strength K_4 [3] and on each site there is a single ion potential D [2]. All these interactions are limited to the first nearest neighbors.

Recent researches of this Ising model and its phase diagrams with four spin interaction and some of its applications have been done [4–8].

The selenium compound adsorbed on a nickel surface [9] is a good physical picture for this model. Different methods have been used to understand the critical behaviour of this model. For the two dimensional case, all of mean-field approximation (MFA) [10–13] Monte Carlo simulations (MC) [11–14], series analysis [15], exact duality [16], transfer-matrix finite size scaling calculations [9, 14, 17], renormalization group [18, 19] and mean field renormalization group approach [20], yield three different phases: a paramagnetic phase in which neither σ nor S nor anything else is ordered ($\langle \sigma \rangle = \langle S \rangle = \langle \sigma S \rangle = 0$); Baxter phase in which σ and S independently order in ferromagnetic fashion, and also $\langle \sigma S \rangle \neq 0$; a third phase called PO_1 in which σS is ferromagnetically ordered $\langle \sigma S \rangle \neq 0$ but $\langle \sigma \rangle = \langle S \rangle = 0$.

One of the most interesting and challenging phenomena is the appearance of other new partially ordered phases in the ATM. For example, MFA and MC simulations applied to the three-dimensional case yield first and second-order phase transitions and partially ferromagnetic ordered phase $\langle \sigma \rangle$ ($\langle \sigma \rangle \neq 0$ and $\langle S \rangle = \langle \sigma S \rangle = 0$) [11]. By using exact duality transformations and symmetry considerations [17, 21], the anisotropic ATM in $d = 2$ also presents partially ordered phases called $\langle \sigma \rangle$ and $\langle S \rangle$ which are connected by symmetry operations to the $\langle \sigma S \rangle$ phase. These results are confirmed in $d = 2$ and $d = 3$ by MFA and MC simulations [12]. The PO_2 phase defined by ($\langle S \rangle = \langle \sigma \rangle \neq 0$; $\langle \sigma S \rangle = 0$) found in the spin-1 Ashkin-Teller model [14, 22] does not occur in the spin-1/2 Ashkin-Teller model [12].

*raniaboudefla@yahoo.com

Monte Carlo (MC) simulation can be shown as a powerful and successful tool to study critical phenomena [12] at reduced dimensionality ($d = 2$). So, it is of importance to fully understand the phase diagram obtained from this model through a nonperturbative method, such as Monte Carlo technique. The main problem which arises from this method is the existence of statistical errors.

In this paper, we mainly focused on the spin-3/2 Ashkin-Teller model using MC simulations. The paper is organized as follows: in the second section, the investigated model is introduced and the ground state diagram is presented. Section 3 contains the description of the methodology and formalism of the MC simulations. We collect our results and discussions in section 4. Finally, the summary and conclusions are drawn in section 5.

2. Model and ground state diagram

The Hamiltonian of the model can be expressed as:

$$H = -K_2 \sum_{\langle ij \rangle} (\sigma_i \sigma_j + S_i S_j) - K_4 \sum_{\langle ij \rangle} \sigma_i \sigma_j S_i S_j - D \sum_{\langle i \rangle} (S_i^2 + \sigma_i^2), \quad (2.1)$$

where the spins σ_i and S_i are located on sites of an hypercubic lattice and take both the values $\pm 3/2$ and $\pm 1/2$. The first term describes the bilinear interactions between the spins at sites i and j , with the interaction parameter K_2 . The second term describes the four-spins interaction with strength K_4 and on each site there is a single ion potential D . All these interactions are restricted to the z nearest neighbours pairs of spins.

In order to calculate the ground state energy, we express the hamiltonian as a sum of contributions of the nearest-neighbour spins. So, the contribution of a pair S_1, S_2 and σ_1, σ_2 is:

$$E_p = -K_2(\sigma_1 \sigma_2 + S_1 S_2) - K_4 \sigma_1 \sigma_2 S_1 S_2 - D(S_1^2 + S_2^2 + \sigma_1^2 + \sigma_2^2). \quad (2.2)$$

By comparing the values of E_p for different configurations, we obtain the following structure of phase diagram shown in figure 1:

- (i) For $K_4/K_2 < D/K_2$: if $K_4/K_2 < -0.4$, the spins σ_i are parallel while the spins S_i are antiparallel. Then we have: $\langle S \rangle_F = \langle \sigma \rangle_{AF} = \langle \sigma S \rangle_F = 0$ and $\langle S \rangle_{AF} = \langle \sigma \rangle_F = 3/2$ and $\langle \sigma S \rangle_{AF} \neq 0$ which characterize the phase called Baxter-3/2, otherwise if $K_4/K_2 > -0.4$ the Baxter-3/2 phase is stable since both spins σ_i and S_i are aligned and equal to 3/2.
- (ii) For $K_4/K_2 > D/K_2$: if $K_4/K_2 < -4$, the spins σ_i are parallel while the spins S_i are antiparallel. Then we have: $\langle S \rangle_F = \langle \sigma \rangle_{AF} = \langle \sigma S \rangle_F = 0$ and $\langle S \rangle_{AF} = \langle \sigma \rangle_F = 1/2$ and $\langle \sigma S \rangle_{AF} \neq 0$ which characterize the phase called Baxter-1/2. The symbols $\langle \dots \rangle_F$ and $\langle \dots \rangle_{AF}$ indicate the thermal average of spin variables respectively in the ferromagnetic and antiferromagnetic phases, or else if $K_4/K_2 > -4$, the Baxter-1/2 phase is stable since both spins σ_i and S_i are aligned and equal to 1/2.
- (iii) Except for $K_4/K_2 > D/K_2$, in the area $0 < D/K_2 < -1$, two Baxter mixed phases have been found, the first when $K_4/K_2 > -0.4$, all the spins σ_i and S_i are parallel, and the second one if $K_4/K_2 < -0.4$, the spins S_i are parallel while the spins σ_i are misaligned.

3. Monte-carlo simulations

The system studied here is a $L \times L$ square lattice with even values of L , containing $N = L^2$ spins. In order to update the lattice configurations, the well-known Metropolis algorithm [12] is used with periodic boundary conditions. Monte-Carlo (MC) simulations are performed for $d = 2$ with systems of sizes $L = 10, 16, 20, 30, 40$ and 60 . We use 100000 to 200000 MC steps to calculate the thermodynamic quantities after discarding 5000–50000 sweeps for thermal equilibrium. Most of the phase diagrams presented here are

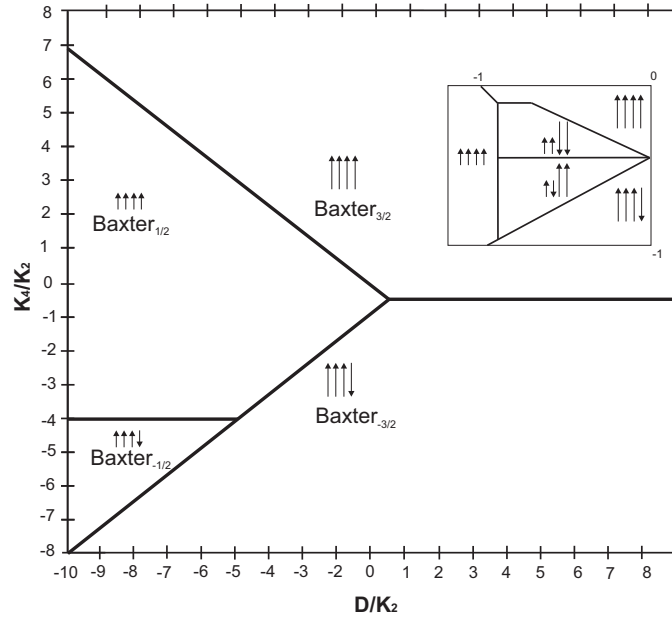


Figure 1. Ground state phase diagram.

obtained with $L = 30$. The physical quantities of use are the magnetizations $|M_\alpha|$ ($\alpha = \sigma, S, \sigma S$), and are estimated by:

$$|M_\alpha| = \langle |M_\alpha| \rangle = \frac{1}{Np} \sum_c \sum_i \alpha_i(c) \quad \text{with} \quad \alpha = \sigma, S, \sigma S, \quad (3.1)$$

where i runs over the lattice sites, c runs over the configurations obtained to update the lattice over one sweep of the N spins of the lattice [one Monte-Carlo step (MCS)] counted after the system reaches thermal equilibrium, and p is the number of the MCS. In order to measure the phase boundaries, we find useful the measurement of fluctuations (variance of the order-parameters) in M_α defined by the magnetic susceptibility:

$$\chi_\alpha = \frac{N}{k_B T} (\langle M_\alpha^2 \rangle - \langle |M_\alpha| \rangle^2) \quad \text{with} \quad \alpha = \sigma, S, \sigma S, \quad (3.2)$$

k_B is the Boltzmann's constant.

4. Results and discussion

The phase diagram obtained by Monte Carlo simulation is shown in figure 2 and presented in the plane $(k_B T/K_2, D/K_2)$. We have a paramagnetic phase, where $\langle \sigma \rangle = \langle S \rangle = \langle \sigma S \rangle = 0$ and two ferromagnetic (Baxter) phases, where $\langle \sigma \rangle$ and $\langle S \rangle$ are ordered ferromagnetically and also $\langle \sigma S \rangle \neq 0$. The first is Baxter-1/2 and the second is the Baxter-3/2 which were not found in the earlier works [13, 14]. These phases are separated by critical lines, multicritical points and two partially ordered phases: the $\langle \sigma S \rangle$ phase where $(\langle \sigma S \rangle \neq 0$ and $\langle \sigma \rangle = \langle S \rangle = 0)$ and the $\langle S \rangle$ phase where $(\langle \sigma \rangle = \langle \sigma S \rangle = 0, \langle S \rangle \neq 0)$. However, the MC data are obtained from peaks in the susceptibilities [23] for $L = 30$. The nature of the transition is determined from discontinuities (continuities) in the order parameters for first (second) order transition by MC simulations [12]. In our paper, the nature of the transitions is always of second order for all values. We have located the phase boundaries by using the maximum of the susceptibility. This method has been successfully applied to other models [13] and has shown a good precision with the transfer matrix finite-size-scaling method [14].

The results of figure 2 are obtained for $K_4 = 0.25$. We also see the Baxter-1/2 phase separated from the paramagnetic phase by the partially ordered phase $\langle \sigma S \rangle$ at low values of D/K_2 , as seen in the figures 3, 4 and the Baxter-3/2 phase is separated from the paramagnetic phase by the new partially ordered phase

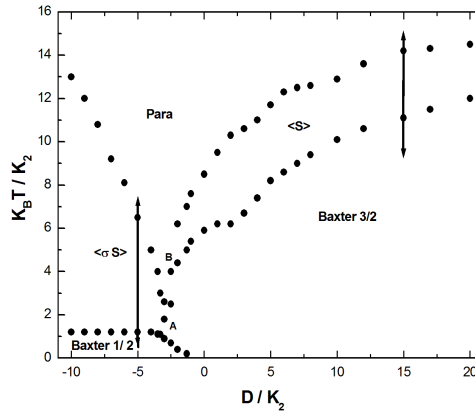


Figure 2. Phase diagram in the $(D/K_2, T/K_2)$ plane for $K_4 = 0.25$ from Monte Carlo simulation, data are shown with $L = 30$.

$\langle S \rangle$ at high values of D/K_2 , as seen in the figures 5, 6. This phase does not exist either in the spin-1/2 [12] or in the spin-1 [14] Ashkin-Teller model but is viewed in the mixed (ATM) [13]. The meeting of all critical lines is located at the multicritical points $A(-2.98 \pm 0.01; 0.77 \pm 0.01)$ and $B(-2.54 \pm 0.01; 3.97 \pm 0.01)$. The two phases $\langle \sigma S \rangle$ and $\langle S \rangle$ separate the disordered phase from the ferromagnetic Baxter phases by second order transition lines.

For error bars, we have made 300000 MCS and discarding 50000 and made measurements every 100 MCS, we plotted errors to the magnetizations and susceptibilities, as seen in the figures 3–6 which present plot of the three order-parameters σ , S and σS as function of temperature for $K_4 = 0.25$ and $D = -5$ (and $D = 15$) as obtained by MC simulations showing that the error bars are very small, the simulation was too long, it took a lot of computing time.

By increasing the four body interaction, K_4/K_2 , the two Baxter phases remain in the phase diagrams whereas depending on the strength of K_4 , as shown in figure 7 for $K_4 = 2$, the partially ordered phase $\langle \sigma S \rangle$ shrinks and the other one $\langle S \rangle$ disappears. But for strong K_4 , $K_4 = 6$, the partially ordered phase $\langle \sigma S \rangle$ disappears and the other partially phase $\langle S \rangle$ is recovered as shown in figure 8. Continuous lines are

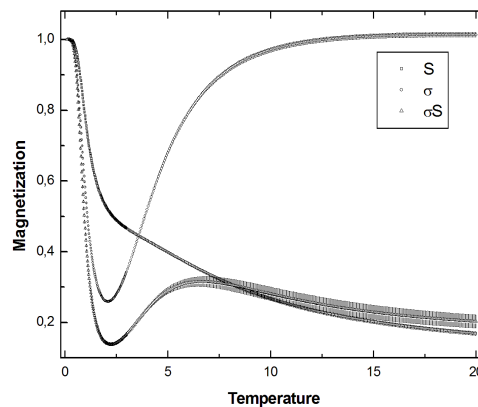


Figure 3. Plot of the three order-parameters $\langle \sigma S \rangle$, $\langle \sigma \rangle$ and $\langle S \rangle$ with error bars as function of temperature for $K_4 = 0.25$ and $D = -5$ as obtained by MC simulations for the square lattice showing that the phase transitions are of second-order.

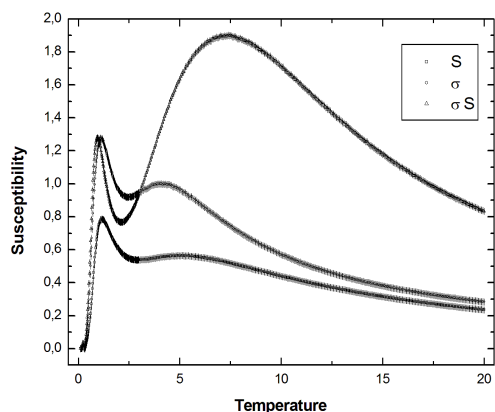


Figure 4. Plot of the susceptibility with error bars for $K_4 = 0.25$ and $D = -5$ as functions of temperature showing the existence of the phase $\langle \sigma S \rangle$, where at $T_1' = 1.20$, $\langle \sigma S \rangle \neq 0$ and $\langle \sigma \rangle = \langle S \rangle = 0$, whereas at $T_1'' = 6.48$ we have $\langle \sigma \rangle = \langle S \rangle = \langle \sigma S \rangle = 0$.

linked by multicritical points of higher order.

5. Conclusion

In this paper, by using MC simulations we have shown that the isotropic ferromagnetic Ashkin-Teller model presents a new partially ordered phase $\langle S \rangle$, which is very clear at high temperatures (also found infinitesimal in the Monte Carlo mixed ATM [13]), and other phases like Baxter-3/2 where all spins have the magnitude of 3/2. In the parameter space $(K_4/K_2, D/K_2$ and $T/K_2)$, the phase diagrams present rich varieties of phase transitions with surfaces of second order phase transitions, bounded by lines of multicritical points.

In conclusion, the study was carried out on the model of Ashkin-Teller spin-3/2. It has revealed the complexity of the model with very rich structures and gives a better understanding of the properties

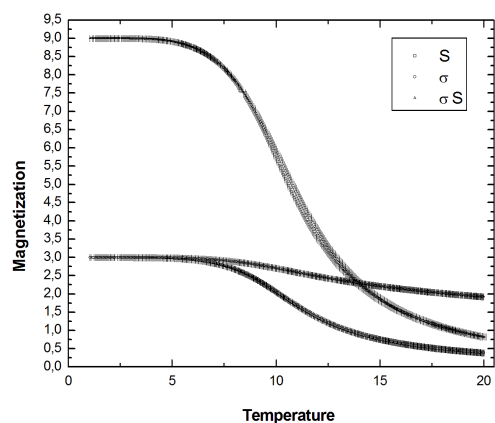


Figure 5. Plot of the three order-parameters $\langle \sigma S \rangle$, $\langle \sigma \rangle$ and $\langle S \rangle$ with error bars as function of temperature for $K_4 = 0.25$ and $D = 15$ as obtained by MC simulations for the square lattice showing that the phase transitions are of second-order.

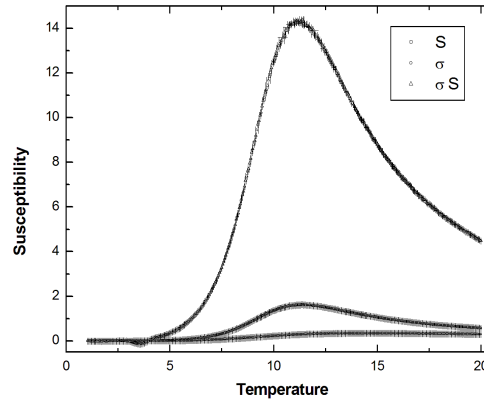


Figure 6. Plot of the susceptibility with error bars for $K_4 = 0.25$ and $D = 15$ as functions of temperature showing the existence of the phase $\langle S \rangle$, where at $T_2^I = 11.10$, $\langle \sigma \rangle = \langle \sigma S \rangle = 0$, $\langle S \rangle \neq 0$, whereas at $T_2^{II} = 14.21$ we have $\langle \sigma \rangle = \langle S \rangle = \langle \sigma S \rangle = 0$.

of condensed matter, especially magnetic properties of the systems consisting of many atom molecules holders. It is on the basis of this study that we plan to study the magnetic properties of the Ashkin-Teller model with mixed spins on different types of lattices. The presence of many atoms with different magnetic moments on the same site can reveal some interesting properties. The model will also be analyzed in three dimensions including the crystal fields and long range interactions.

References

1. Ashkin J., Teller E., Phys. Rev., 1943, **64**, 178; doi:10.1103/PhysRev.64.178.
2. Kogut J.B., Rev. Mod. Phys., 1979, **51**, 659; doi:10.1103/RevModPhys.51.659.
3. Barreto F.C.S., Braz. J. Phys., 2013, **41**, 43; doi:10.1007/s13538-012-0104-z.
4. Chatelain C., Condens. Matter Phys., 2011, **17**, 33601; doi:10.5488/CMP.17.33601.
5. Huang Y., Deng Y., Jacobsen J.L., Salas J., Nucl. Phys. B, 2013, **868**, 492; doi:10.1016/j.nuclphysb.2012.11.015.
6. Chang Z., Wang P., Zheng Y.-H., Commun. Theor. Phys., 2008, **49**, 525; doi:10.1088/0253-6102/49/2/57.

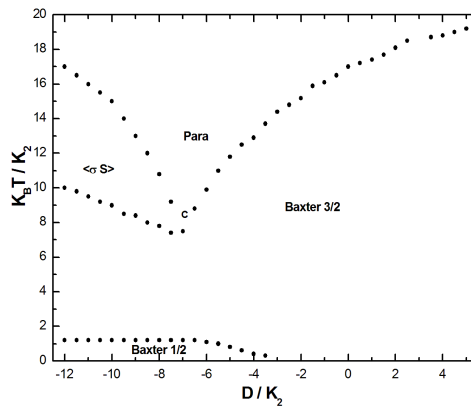


Figure 7. Phase diagram in the $(D/K_2, T/K_2)$ plane for $K_4 = 2$ from Monte Carlo simulation, data are shown with $L = 30$.

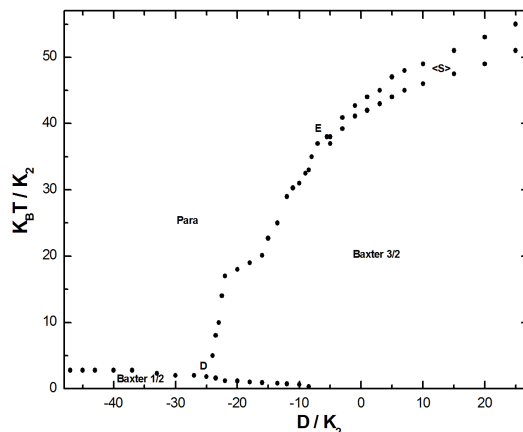


Figure 8. Phase diagram in the $(D/K_2, T/K_2)$ plane for $K_4 = 6$ from Monte Carlo simulation, data are shown with $L = 30$.

7. Le J.-X., Yang Zh.-R., Commun. Theor. Phys., 2005, **43**, 841; doi:10.1088/0253-6102/43/5/017.
8. Bezerra C.G., Mariza A.M., de Araújo J.M., da Costa F.A., Physica A, 2001, **292**, 429; doi:10.1016/S0378-4371(00)00568-9.
9. Bak P., Kleban P., Unertel W.N., Ochab J., Akinci G., Barlet N.C., Einstein T.L., Phys. Rev. Lett., 1985, **54**, 1542; doi:10.1103/PhysRevLett.54.1539.
10. Zhang G.M., Yang C.Z., Phys. Rev. B, 1993, **48**, 9452; doi:10.1103/PhysRevB.48.9452.
11. Ditzian R.V., Banavar J.R., Grest G.S., Kadano L.P., Phys. Rev. B, 1980, **22**, 2542; doi:10.1103/PhysRevB.22.2542.
12. Bekhechi S., Benyoussef A., Elkenz A., Ettaki B., Loulidi M., Physica A, 1999, **264**, 503; doi:10.1016/S0378-4371(98)00474-9.
13. Bekhechi S., Benyoussef A., Elkenz A., Ettaki B., Loulidi M., Eur. Phys. J. B, 2000, **18**, 278; doi:10.1007/s100510070058.
14. Badehdah M., Bekhechi S., Benyoussef A., Ettaki B., Phys. Rev. B, 1999, **59**, 6250; doi:10.1103/PhysRevB.59.6250.
15. Ditzian R.V., Phys. Lett. A, 1972, **38**, 451; doi:10.1016/0375-9601(72)90032-1.
16. Wegner F.J., J. Phys. C: Solid State Phys., 1972, **5**, L131; doi:10.1088/0022-3719/5/11/004.
17. Badehdah M., Bekhechi S., Benyoussef A., Touzani M., Physica B, 2000, **291**, 394; doi:10.1016/S0921-4526(00)00279-9.
18. Banavar J.R., Jasnow D., Landau D.P., Phys. Rev. B, 1979, **20**, 3820; doi:10.1103/PhysRevB.20.3820.
19. Knops H.J.F., J. Phys. A: Math. Gen., 1975, **8**, 1508; doi:10.1088/0305-4470/8/9/020.
20. Plascak J.A., Sa Barreto F.C., J. Phys. A: Math. Gen., 1986, **19**, 2195; doi:10.1088/0305-4470/19/11/027.
21. Wu F.Y., Lin K.Y., J. Phys. C: Solid State Phys., 1974, **7**, L181; doi:10.1088/0022-3719/7/9/002.
22. Loulidi M., Phys. Rev. B, 1997, **55**, 11611; doi:10.1103/PhysRevB.55.11611.
23. Ditzian R.V., J. Phys. C: Solid State Phys., 1972, **5**, L250; doi:10.1088/0022-3719/5/17/005.

Чисельне вивчення спінів-3/2 моделі Ашкіна-Теллера

Р. Будефля¹, С. Бекеші¹, Ф. Гонтінфінде²

¹ Лабораторія теоретичної фізики, В.Р. 230, Університет Абу Бакр Белькаїд, Тлемсен 13000, Алжир

² Відділення фізики (FAST) та інститут математики і фізичних наук (IMSP), Університет Абомей-Калаві, Бенін

Вивчення моделі Ашкіна-Теллера спінів-3/2 на гіперкубічній ґратці здійснюється методом Монте Карло. Продемонстровано фазові діаграми і обговорено простір фізичних параметрів. Виявлено багатство фізичних властивостей, а саме, перехід другого роду і мультикритичні точки. Фазові діаграми отримані шляхом зміни сили, що описує чотириспінову взаємодію та одноіонний потенціал. Дана модель демонструє нову високотемпературну частково впорядковану фазу, що називається $\langle S \rangle$, і новий основний 3/2 стан Бакстера, якого нема в моделях Ашкіна-Теллера спінів-1/2 і spin-1.

Ключові слова: моделювання, Ашкін-Теллер, спінів-3/2, Монте-Карло, фазова діаграма, Бакстер